

Modeling Radiation-Induced Transients in the Next Generation Space Telescope (NGST)

James C. Pickel
PR&T
1997 Katie Ct.
Fallbrook, CA 92028
jim@pickel.net
Robert Reed, Ray Ladbury
NASA/GSFC
Bernie Rauscher
STScI
Paul Marshall
Consultant-NASA/GSFC
Tom Jordan
EMP Consultants
Bryan Fodness, George Gee
SGT, Inc.

Abstract— The Next Generation Space Telescope (NGST) mission has extremely low noise requirements, on the order of a few electrons, combined with very long integration times on the order of 1000 seconds. The telescope will operate in an L2 orbit and will be exposed to the galactic cosmic rays and solar flare radiation environments. As a risk reduction measure, the project is performing a radiation effects assessment of the impact of ionizing transients in the FPA on the science goals. This paper summarizes our approach to the assessment of radiation-induced transients and describes recent progress in model development.

NGST	Next Generation Space Telescope
NICMOS	Near Infrared Camera and Multi-Object Spectrometer
NIR	near infrared
NOVICE	Monte-Carlo transport code
PV	photovoltaic
ROIC	readout integrated circuit
SCA	sensor chip assembly
SPE	solar particle event
TRIM	Transport of Radiation In Matter (transport code)

TABLE OF CONTENTS

1. INTRODUCTION
2. APPROACH
3. RADIATION ENVIRONMENT
4. RADIATION TRANSPORT ANALYSIS
5. FPA INTERACTION MODEL
6. CONCLUSIONS

GLOSSARY OF TERMS

APS	active pixel sensor
CAD	computer aided design
CCD	charge coupled device
EASY	Activation and decay code
FPA	focal plane array
GCR	galactic cosmic ray
GEANT	Monte-Carlo transport code
GSFC	Goddard Space Flight Center
IBC	impurity band conduction
IRFPA	infrared focal plane array
ISO	Infrared Space Observatory
L2	second Lagrange point
LET	linear energy transfer
MCNP	Monte Carlo N-Particle (transport code)
MIR	mid infrared
MOSFET	metal-oxide-silicon field effect transistor

1. INTRODUCTION

The Next Generation Space Telescope (NGST) is currently in the system concept definition phase, with preliminary designs underway. NGST is planned to be launched in 2009 and will be placed in orbit at the Second Lagrange point (L2). The science mission includes high resolution imaging and spectroscopy in a near infrared (NIR) wavelength band with cut-off wavelength of $\sim 5 \mu\text{m}$ and cut-on wavelength of $\sim 0.6 \mu\text{m}$. The mid infrared band (MIR) will have a cut-off wavelength of $\sim 28 \mu\text{m}$. The NIR focal plane array (FPA) is currently planned as a 4k x 4k layout comprised of four 2k x 2k butted sensor chip assemblies (SCA). The NIR detectors will be either InSb or HgCdTe photovoltaic (PV) detectors operated in the range of 30 – 40 K. The MIR FPA is currently planned as a 1k x 1k FPA having four electrically independent outputs. The MIR detectors will be impurity band conduction (IBC) arsenic-doped silicon (Si:As) detectors operated in the range of 7 – 10 K.

A preliminary estimate is that one practical limit to exposure times will be about 1000 seconds. This limit is set by cosmic ray flux and envisions that cosmic rays will be rejected from astronomical scenes by stacking sets of dithered 1000 seconds-long exposures on the ground.

Longer exposure time may be possible using more sophisticated ground-based cosmic ray rejection software to identify hits and continue the integration. Under this

paradigm, each pixel would be sampled non-destructively several times as charge accumulates. Intermediate samples would be down-linked to the ground, and powerful ground-based software would identify hits and fit a slope using knowledge of hits to reject them. Although this approach has worked well with NICMOS, it has not yet been empirically demonstrated at the noise levels required for NGST.

The science mission requires a combination of very low noise (10 electrons) and very long integration times (1000 seconds). These requirements place unprecedented demands on performance with respect to transient radiation effects from the space environment. The ionizing particle environments of concern include galactic cosmic rays (GCR) and solar particle event (SPE) generated protons and heavy ions. In addition, inherent and induced radioactive sources in the material surrounding the FPA is a concern.

A program is underway at NASA Goddard Space Flight Center (GSFC) to assess the radiation effects on the proposed NGST designs and guide mission planning. Preliminary estimates indicate that total ionizing dose damage and displacement damage are not likely to be a problem for the NGST FPA technologies. This will be verified experimentally. The current emphasis of the study is the potential for ionizing-particle-induced transients from energetic penetrating ions to compromise the FPA noise.

While there are established software / data processing approaches to mitigate the large transients due to primary particles, small transients on the order of the noise floor of 10 electrons cannot be distinguished, and unavoidably contribute to the noise in the data. Control of integration time is one approach to manage the low level transient induced noise, however the goal of the science mission is to achieve an integration time of 1000 seconds. A detailed modeling and experimental program is being performed to predict the radiation-induced transients in the proposed NGST FPA during orbit. This paper summarizes the current state of the modeling and outlines future work.

2. APPROACH

The ionizing transients arise from several sources including primary cosmic rays, secondary particles from interactions in material surrounding the FPA, and radioactivity in the surrounding material from activation and from radioactive contaminants. The assessment consists of three major activities -- determining the local ionizing particle environment at the FPA, determining the FPA response to the environment, and assessing the impact on science mission performance for various operational scenarios. Figure 1 shows a block diagram of the overall assessment approach.

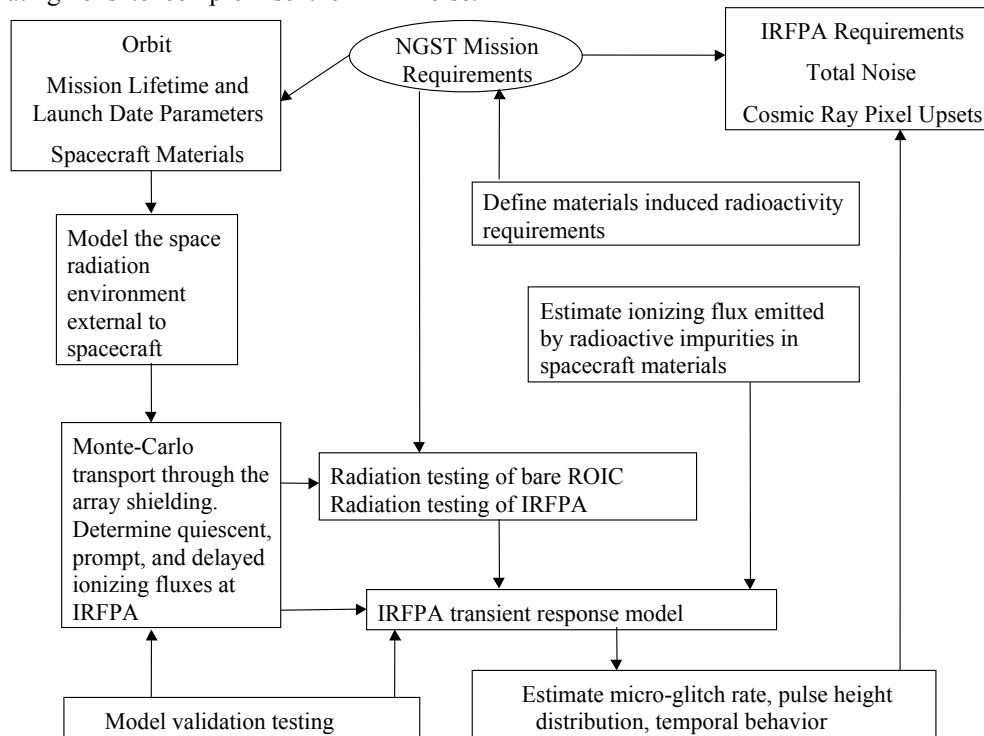


Figure 1. Approach for transient radiation effects assessment.

We are performing detailed Monte-Carlo transport analyses to define the ionizing particle environment at the FPA. Concerns for very small transients and pixel-upset

specifications require that the transport codes track low-energy secondary particles as well as primary particles. Several codes are being used including MCNP/MCNPX,

GEANT4, NOVICE, and EASY. A FPA interaction model is being developed to predict the spatially-dependent charge contamination on a pixel-by-pixel basis. The array model divides the charge collection into depletion regions for each pixel and a common diffusion regions. Both the detector layer and the readout integrated circuit layer are included. Incident particle events are characterized by the type of particle, energy, hit location on the surface of the FPA and angle of incidence. The charge generated in the FPA material is then distributed to the appropriate pixels to produce a pixel map of charge contamination events. The charge contamination pixel maps will be combined with pixel dark-field noise maps and imaging scenes to assess the performance impact. Predictions of FPA transients will be made for various operational scenarios including integration time, solar weather, FPA design and spacecraft design.

3. RADIATION ENVIRONMENT

Primary Particles

The ionizing particle environment at L2 consists of protons and heavy ions from GCR and SPE sources. The elemental composition of the primary GCR particles is 77% protons, 21% alphas, with smaller amounts of the remaining elements. The GCR environment is continuous, with a modest modulation over the 11 year solar cycle. The SPE environment is composed primarily of protons but can also contain heavy ions. The SPE environment is stochastic in nature and can vary by many orders of magnitude. There is no requirement to operate during a flare, however there is concern for residual induced radioactivity following a flare. Operation could be limited until the radioactivity has decayed.

Secondary Particles

The principal energy loss mechanism for primary protons and heavy ions is weak Coulombic interaction with bound electrons of the target material, resulting in ionization. Electrons are raised to the conduction band in semiconductors but are still bound to the host atom. For some Coulombic interactions, relatively larger amounts of energy are transferred, and the energetic electrons travel away from the host atom and become a source of further ionization at locations remote from the primary particle track. Such energetic electrons that escape the host atom are termed delta electrons. If a primary particle interacts with a nucleus of the target, energetic secondary particles (protons, neutrons or ions) can be ejected and initiate a series of cascade events that cause ionization at locations away from the primary track. The modeling problem is to predict the spatially-dependent energy depositions (ionization) in the various pixels of the FPA from both the primary particle tracks and the secondary particles. The approach is to perform transport analysis of the primary particle environment through the material surrounding the detector, and to perform charge deposition analysis of the

primary and secondary particles that reach the sensitive charge collection volumes in the FPA.

There is experimental evidence of secondary particles interfering with IR telescopes from the on-orbit experience of the European Space Agency's Infrared Space Observatory (ISO) [1]. Measurement of transients in the ISO detectors indicated a transient rate approximately 80 % higher than could be accounted for by the primary particles. The higher than expected transient rate was attributed to secondary particles and delta electrons.

Activation and Inherent Radioactivity

The penetrating radiation through the spacecraft can cause the structure to become radioactive by inducing nuclear reactions that yield unstable activation products throughout satellite structures. The aggregate increase in radiation levels due to this induced activation will be a complex function of the cosmic ray and solar proton environments, the elemental makeup of the materials throughout the satellite, the location in the satellite, and time. Temporal variations in the induced activity levels occur due to variations in both the buildup and decay rates. The buildup will begin as soon as the observatory is launched and the cosmic ray environment is encountered. Since there may be many important activation products, the buildup will be complex, even if the external environment is invariant (which it is not). Each unstable activation product species will interact with its local environment by producing photons and/or particle radiation at a rate governed by an exponential decay process and a half-life that is characteristic of the nuclide in question. Equilibrium rates will be approached for activation byproducts that are short-lived relative to their production rates, but the activity levels of activation products with half-lives of months or years will increase over the duration of the mission. Therefore, we would expect an increasing transient rate over the duration of the mission. Superimposed on this temporal behavior governed by the cosmic ray induced activity, there will be very dramatic increases in the inventories of activation products when solar particle events occur. One of our key concerns is that the induced radiation activity levels may be so high immediately following major solar particle events, that the NGST science mission will be compromised for a period of days or longer.

Another spacecraft-generated source of ionizing radiation is inherent radioactive impurities contained in spacecraft materials. For example, Beryllium, unless it is processed using special techniques, will contain trace levels of radioactive Uranium that will contribute to the FPA noise rate. Also, optical glasses that utilize high-Z elements for refractive index control are known sources for contamination from Thorium decay products. This source can be managed by careful selection and possible screening of materials used near the FPA.

4. RADIATION TRANSPORT ANALYSIS

Models of the GCR environment and the SPE environment are established for the L2 orbit [2]. Transport analysis is being performed with the external environments for various possible materials that will be in the vicinity of the FPA to predict the primary and secondary particle environments that reach the FPA. Preliminary results are being obtained using a spherical shell geometry with various materials to gain an understanding of the impact of material variations on the secondary particle environment. The NGST telescope geometry is being modeled in detail using computer aided design (CAD) data. Particular attention is being paid to the details of the materials and geometry in the immediate vicinity of the FPA, including coatings, epoxies, mounting boards, etc. The transport analysis will ultimately be performed for the detailed telescope geometry.

No single transport code is optimized for the requirements of this assessment. Consequently we are employing several codes to attack the various aspects of the problem.

Candidate codes for our purposes include:

- MCNP/MCNPX – MCNP was originally developed by the nuclear community to model propagation of

neutrons, electrons and photons in matter. MCNPX extends capabilities to protons, etc.

- GEANT4 – originally developed at CERN to model passage of particles through particle detectors.
- NOVICE – developed by Tom Jordan to perform extremely accurate spacecraft shielding calculations.
- EASY - being assessed to establish time and solar particle activity dependent source terms for activation products and subsequent unstable decay products.

All of these Monte Carlo codes have been previously validated against experiment by numerous investigators.

5. FPA INTERACTION MODEL

The overall transient noise problem for the sensor in the space environment is illustrated in Figure 2, showing the FPA enclosed in surrounding material (packaging, telescope, spacecraft, etc.). The primary particles penetrate the FPA, as well as secondary particles from interactions within the surrounding material, induced radioactivity, and inherent radioactivity. We note that the secondary particles and delta electrons are time-coincident with the primary particles, since they are generated by the primaries. This fact simplifies the mitigation strategy since the primary particles are typically large enough to be detected. We also note that the secondary particles and delta electrons have a limited range.

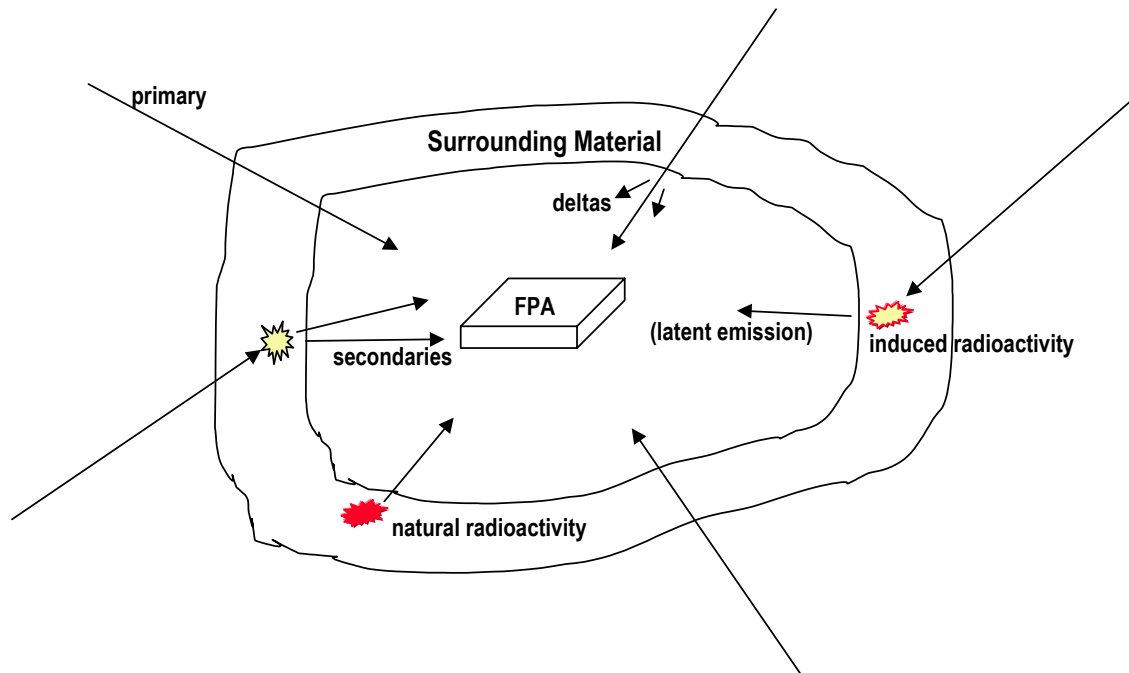


Figure 2. Ionizing particle radiation incident on the FPA.

The FPA interaction model has basis from a similar approach used by Lomheim and co-workers to predict proton-induced charge deposits in CCDs [3,4]. The

model accounts for the variation of charge collection in each pixel of the hybrid FPA following charge generation along the path of an ionizing particle, either electrons, protons or heavy ions. The model specifically addresses

the 3-D geometry of charge collection volumes in a hybrid FPA, consisting of an array of detectors hybridized to a readout integrated circuit (ROIC) array through indium bump interconnects. Figure 3 shows a cross-section of a typical HgCdTe hybrid FPA. The CdTe substrate may be thinned or removed. A similar structure is used for InSb detectors with the substrate removed.

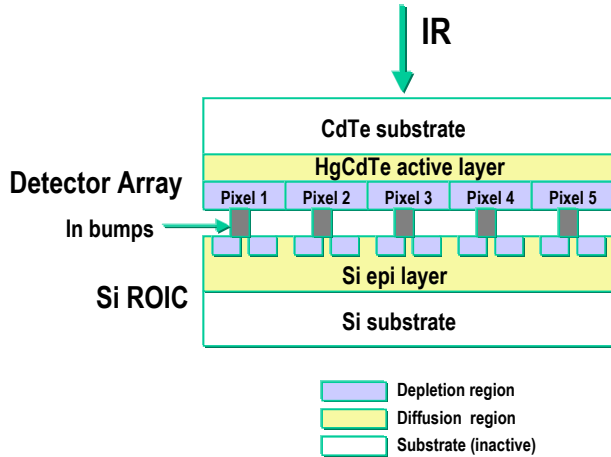


Figure 3. Typical hybrid IR FPA geometry. A detector array is hybridized to a Si ROIC through Indium bump bonds. Charge collection due to the passage of ionizing particles occurs in both the detector array and the ROIC array.

The model output is a pixel map of charge deposits across the FPA due to the particles that strike the FPA during the integration time. This data can then be combined with a device-dependent distribution of inherent noise to produce a simulated “dark image” file.

The charge collection volumes (sensitive volumes) associated with a particular pixel are defined as those regions that collect charge to the integration capacitance for the pixel. The sensitive volumes in the photovoltaic detectors consist of the depletion volume of the p-n junction and the smaller of either the volume defined by the junction area and the minority carrier diffusion length in the detector active layer, or the pixel area and active layer thickness. The sensitive volumes in the ROIC are defined by the pixel pitch and the thickness of the Si epitaxial layer or the minority carrier diffusion length. The entire pixel volume of both the detector and the ROIC is sensitive to charge collection because the integration time is much longer than minority carrier lifetimes.

A key concern is charge spreading to adjacent pixels from the pixel that is penetrated by the particle, i.e., radiation crosstalk. Figure 4 shows an example of one possible mechanism for charge spreading in the ROIC of a staring FPA. In this example, we show a 5 μm epitaxial layer with a Source/Follower readout in each pixel. The side of the reset MOSFET that is connected to the integration capacitor is a sensitive junction. When charge is collected on the sensitive junction, it is integrated on the integration capacitor. The integration time is long compared to minority carrier diffusion times. Thus, all charge that diffuses from the ion path to any sensitive junction will be collected and counted to the respective pixel. In order to accurately model the charge collection by diffusion, the field assisted drift component associated with the MOSFETs needs to be taken into account. Similar considerations for charge spreading by diffusion apply to CCD, active pixel sensor (APS) and photovoltaic (PV) detector technologies.

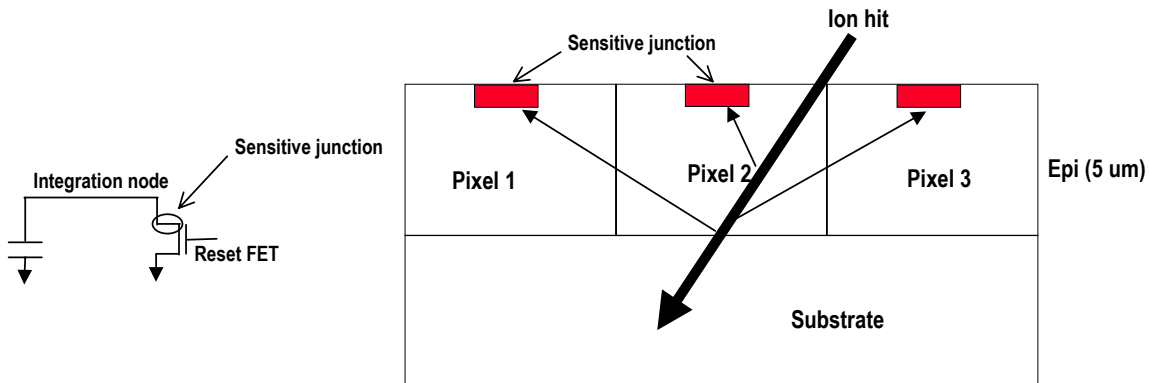


Figure 4. A possible mechanism for charge spread by diffusion in the ROIC.

The modeling task is to calculate charge generation along the 3-D path of the particle and follow each generated carrier until it is collected on a pixel integration node or it recombines.

For the current version of the model, we are not addressing temporal variation of charge collection. This omission is justified since integration times (1000 seconds) are much longer than charge collection times (nanoseconds). The final result is a mapping of predicted

charge collection across the array during the integration time.

Figure 5 illustrates the model. Such a model can be applied to any detector structure, even complex hybrid

FPA's, by registering the various layers on the Cartesian coordinate system and propagating the particle trajectory through the structure.

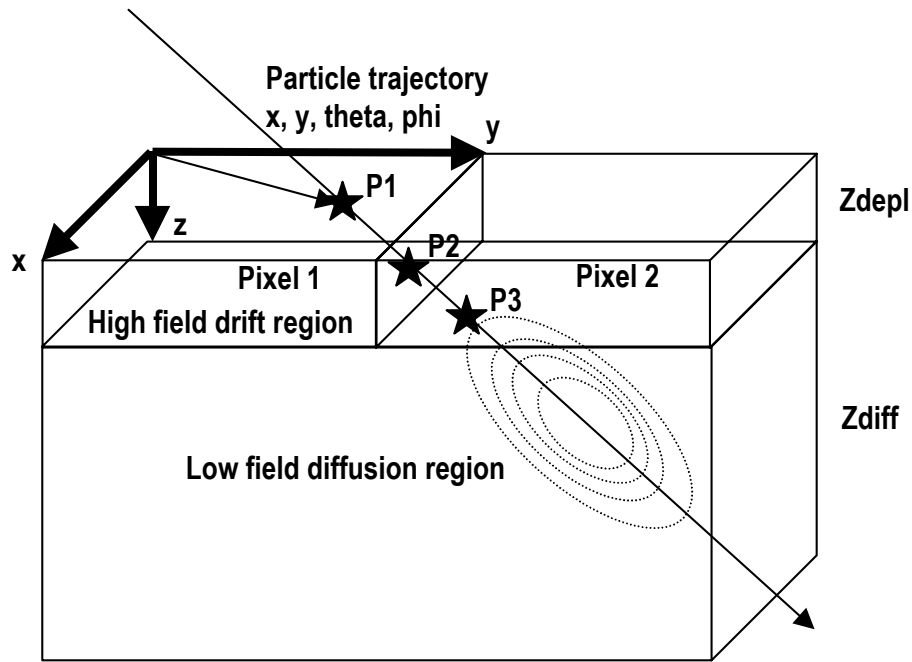


Figure 5. Illustration of Array Charge Model. A particle passes through depletion regions in pixel 1 from P1 to P2, and pixel 2 from P2 to P3 and then passes into the common substrate diffusion region.

The source term for the charge collection model is derived from the external particle environment transported through the material surrounding the FPA. The result of the transport analysis is a list of particles incident on the FPA during the integration time. The particles include both primary and secondary particles and are described with attributes as listed in Table 1.

Table 1. Incident Particle Attributes

Parameter	Symbol	Characteristics
Impact Position	X,Y	Random
Trajectory	Θ, Φ	Isotropic
Particle	Z,A	Depends on primaries, secondaries, radioactive decay
Energy	E	Conforms to energy spectrum at FPA after transport
Stopping Power	LET	Depends on Z, E
Range	R	Depends on Z,E

Table 2 lists the attributes of the FPA that determine the charge collection characteristics. The particle type and

energy determine the linear energy transfer (LET). From the ionization energy for the target material, we can then determine the charge generation rate (carriers/ μm). Recombination of carriers is taken into account by assigning an effective diffusion length. As the particle loses energy to the target material, the energy decreases and the LET changes. The model accounts for this effect by recalculating the energy after each path increment and using an interpolated look-up table of LET versus energy based on the TRIM code [5].

Table 2. FPA Attributes

Parameter	Symbol	Characteristics
Material	InSb, HgCdTe or Si	Determines ionization rate
Pitch		Determines pixel geometry
Depletion Width	Zdepl	Collection by drift
Diffusion Width	Zdiff	Collection by diffusion
Diffusion Length	Ldiff	Limits diffusion

Assumptions

The modeling goal is to determine the final spatial charge distribution across the array with the highest fidelity possible. Since noise levels on the order of 10 electrons are of concern, we are operating at levels much lower than are normally considered for radiation effects analysis. An exact accounting of the fate of each free carrier generated in the array (up to 2k x 2k) during the 1000 second integration period is not computationally practical. Thus, we make several simplifying assumptions and utilize a combination of modeling approaches.

The path of high energy protons and heavy ions is assumed to be a straight line through the FPA (array of detector pixels geometrically registered to array of ROIC unit cells), with trajectory determined by the initial angle of incidence (θ, Φ) and point of impact (x, y). This assumption is justified since the ions are deviated from their path only by nuclear scattering and this is low probability in the small dimensions of the FPA.

However, the path of electrons is not straight within FPA dimensions because electrons are scattered by collisions with bound electrons in the target material. To account for the zigzag path of the electrons, we use the Monte Carlo routines in the NOVICE code [6].

Each particle has a residual range that is determined by its energy. If a particle range is less than the remaining distance within the current pixel, the particle energy and resulting charge is assumed to be deposited at that point.

Energetic secondary electrons (delta electrons) are generated along the path of protons or heavy ions by Columbic interactions that transfer energy to valence electrons in the target material. The delta electrons are a source of further ionization and charge deposition. We account for delta electron generation within the FPA assembly (active side of detector, interconnecting indium bump-bonds, and active side of ROIC) with a source generation function pre-calculated with the NOVICE code for each material of interest.

Secondary particle production from nuclear scattering is neglected since the probability is small.

Energy deposition determined by LET is converted to charge deposition through the ionization energy for the target material. For HgCdTe and InSb with 5 μm cutoff wavelength, the ionization energy is ~ 1 eV per carrier pair (eV/cp). For Si the ionization energy is 3.8 eV/cp at the temperature of interest.

Charge generated within a depletion region of a p-n junction of a PV detector or a high field region in an impurity band conduction (IBC) detector is transported by drift and we assume 100% collection efficiency to the

associated pixel. Charge generated in low field regions within a diffusion length of high field collection regions is transported by diffusion. The current prototype version of the model uses an analytical solution to the 3-D diffusion equation developed by Kirkpatrick to calculate the geometric distribution of charge to the pixel regions [7], similar to the approach used by Lomheim [3].

In a future version of the model, we plan to incorporate a Monte Carlo solution to the charge collection by diffusion. This improvement is necessary to obtain the desired high fidelity and low charge values because there is considerable spatial variation of electric field in the vicinity of the charge collection volumes. While the analytic solution inherently assumes a sharp divide between high-field regions with 100% collection efficiency and low-field diffusion regions, the Monte Carlo approach will account for drift-assisted diffusion in the spatially variant field regions. This aspect of the modeling is currently in development.

Implementation

In practice, modeling of an entire array proceeds by sequentially performing charge deposit calculation in smaller subarrays, using stochastic-based impact particle files, and combining the subarray results to build up the total array results. Particles that pass the boundaries of one subarray are picked up at the appropriate position and trajectory in the adjacent subarray.

We illustrate the modeling approach by describing the program flow as a particle penetrates the FPA. A particle with defined hit position (x, y), angle of incidence (θ, Φ), type (Z), and energy (E) is incident on the FPA. With this information, a pathlength through the FPA is defined, as well as an initial LET. The code increments the path along the pathlength to a new position (x, y, z). At each position we determine the type of region (depletion, diffusion or recombination) for the current point. If the pathlength is in a depletion region, we also determine the pixel for the current location based on the x, y coordinate and the known pixel pitch. The appropriate charge collection model is applied to calculate a charge increment to each pixel in the subarray. A summation tally is kept for each pixel as the particle's position is incremented through the active region. After each increment, the particle energy is re-evaluated to account for the energy loss in the previous increment and the appropriate LET is assigned for the next increment.

In addition to calculating charge generation and transport along the primary particle path, we also calculate secondary electron production and follow the zigzag path, charge generation and transport for all of the thermal charge generated by the secondary electrons. The secondary electron modeling is performed by routines in the NOVICE code.

The program flow is summarized as follows:

- Read impact data from hit file
- Clear data from previous runs
- Increment R along trajectory
- Determine coordinates of current point (x,y,z)
- Determine which pixel we are in (depends on x and y)
- Determine type of region (depends on z) and branch to proper model
 - Depletion
 - Diffusion
- Combine depletion array and diffusion array
- Write arrays to output

The current model is coded in Visual Basic for Excel.

Example Results

Figure 6 shows example output from the prototype charge collection model. Charge collection in a 10 x 10 array of Si volumes with 1 μm depletion width, 20 μm diffusion width and 30 μm pitch is shown for two ion cases, 20 MeV proton and 200 MeV Fe. The angle of incidence is 60 degrees, going from back to front in the picture.

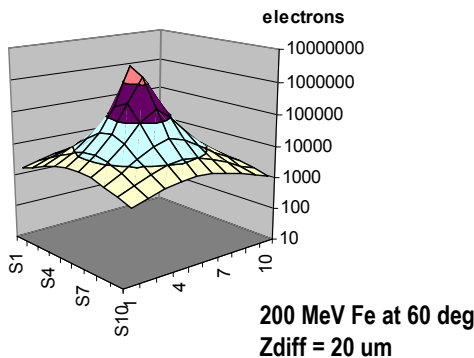
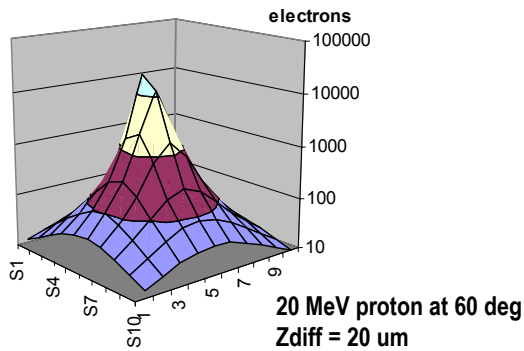


Figure 6. Charge collection in 10x10 array of Si pixels on 30 μm pitch with 1 μm depletion thickness and 10 μm diffusion thickness. Two ion cases are shown.

Figure 7 shows the charge collected in individual pixels after a hit to the center pixel (5,5) of a 10x10 array by a 20 MeV proton incident at 0 degrees. The top picture

shows the charge collected from the depletion regions, the center picture shows the charge collected from the diffusion region and the bottom picture shows the total charge.

20 MeV proton at 0 deg, Zdiff = 10 um

0	0	0	0	0	0	0	0	0	0	0
0	0	0	0	0	0	0	0	0	0	0
0	0	0	0	0	0	0	0	0	0	0
0	0	0	0	0	0	0	0	0	0	0
0	0	0	0	1408	0	0	0	0	0	0
0	0	0	0	0	0	0	0	0	0	0
0	0	0	0	0	0	0	0	0	0	0
0	0	0	0	0	0	0	0	0	0	0
0	0	0	0	0	0	0	0	0	0	0
0	0	0	0	0	0	0	0	0	0	0
0	0	0	0	0	0	0	0	0	0	0

DEPLETION

2	3	4	5	5	5	4	3	2	1
3	5	8	11	13	11	7	5	3	2
4	8	16	33	47	33	16	7	4	2
5	11	33	151	450	142	32	11	5	3
5	13	47	450	8666	403	44	13	5	3
5	11	33	142	403	134	31	11	5	3
4	7	16	32	44	31	15	7	4	2
3	5	7	11	13	11	7	4	3	2
2	3	4	5	5	5	4	3	2	1
1	2	2	3	3	3	2	2	1	1

DIFFUSION

2	3	4	5	5	5	4	3	2	1
3	5	8	11	13	11	7	5	3	2
4	8	16	33	47	33	16	7	4	2
5	11	33	151	450	142	32	11	5	3
5	13	47	450	10074	403	44	13	5	3
5	11	33	142	403	134	31	11	5	3
4	7	16	32	44	31	15	7	4	2
3	5	7	11	13	11	7	4	3	2
2	3	4	5	5	5	4	3	2	1
1	2	2	3	3	3	2	2	1	1

TOTAL

Figure 7. Charge collection in 10x10 array of Si pixels with 30 μm pitch, 1 μm depletion and 10 μm diffusion from a 20 MeV proton at 0 degrees.

Figure 8 shows similar plots for the case of a 20 MeV proton incident at 80 degrees. The proton enters at pixel 5,5 and is traveling toward the bottom of the picture at 80 degrees from the normal. In this case, we note more total charge in the adjacent pixel than the struck pixel because of the large diffusion contribution from the ion track passing underneath.

20 MeV proton at 80 deg, Zdiff = 10 μ m

0	0	0	0	0	0	0	0	0	0	0
0	0	0	0	0	0	0	0	0	0	0
0	0	0	0	0	0	0	0	0	0	0
0	0	0	0	0	0	0	0	0	0	0
0	0	0	0	7424	0	0	0	0	0	0
0	0	0	0	0	0	0	0	0	0	0
0	0	0	0	0	0	0	0	0	0	0
0	0	0	0	0	0	0	0	0	0	0
0	0	0	0	0	0	0	0	0	0	0
0	0	0	0	0	0	0	0	0	0	0

DEPLETION

7	8	11	12	13	12	10	8	6	5
9	13	18	23	24	22	18	13	9	7
14	22	34	49	56	48	33	21	14	9
20	36	70	137	195	135	68	35	19	11
26	55	145	585	20881	550	140	54	25	14
30	71	236	1814	30406	1643	225	69	30	15
30	70	229	1656	13432	1510	218	68	29	15
25	53	132	416	882	399	127	51	25	14
19	33	62	111	142	109	61	33	18	11
13	20	31	42	48	42	30	20	13	8

DIFFUSION

7	8	11	12	13	12	10	8	6	5
9	13	18	23	24	22	18	13	9	7
14	22	34	49	56	48	33	21	14	9
20	36	70	137	195	135	68	35	19	11
26	55	145	585	28305	550	140	54	25	14
30	71	236	1814	30406	1643	225	69	30	15
30	70	229	1656	13432	1510	218	68	29	15
25	53	132	416	882	399	127	51	25	14
19	33	62	111	142	109	61	33	18	11
13	20	31	42	48	42	30	20	13	8

TOTAL

Figure 8. Charge collection from a 20 MeV proton at 80 degrees. (Si, 30 μ m pitch, 1 μ m depletion, 10 μ m diffusion).

Figure 9 shows the case of a 200 MeV Fe ion incident at 0 degrees.

200 MeV Fe at 0 deg, Zdiff = 10 μ m

0	0	0	0	0	0	0	0	0	0	0
0	0	0	0	0	0	0	0	0	0	0
0	0	0	0	0	0	0	0	0	0	0
0	0	0	0	0	0	0	0	0	0	0
0	0	0	0	187000	0	0	0	0	0	0
0	0	0	0	0	0	0	0	0	0	0
0	0	0	0	0	0	0	0	0	0	0
0	0	0	0	0	0	0	0	0	0	0
0	0	0	0	0	0	0	0	0	0	0
0	0	0	0	0	0	0	0	0	0	0

DEPLETION

255	370	519	664	726	660	514	366	251	173
370	611	1004	1498	1753	1483	988	600	364	229
519	1004	2124	4418	6196	4326	2070	980	509	290
664	1498	4418	19989	59796	18871	4236	1453	649	341
726	1753	6196	59796	1.E+06	53503	5882	1695	708	361
660	1483	4326	18871	53503	17856	4151	1438	645	340
514	988	2070	4236	5882	4151	2018	965	504	288
366	600	980	1453	1695	1438	965	590	360	227
251	364	509	649	708	645	504	360	248	171
173	229	290	341	361	340	288	227	171	127

DIFFUSION

255	370	519	664	726	660	514	366	251	173
370	611	1004	1498	1753	1483	988	600	364	229
519	1004	2124	4418	6196	4326	2070	980	509	290
664	1498	4418	19989	59796	18871	4236	1453	649	341
726	1753	6196	59796	1.E+06	53503	5882	1695	708	361
660	1483	4326	18871	53503	17856	4151	1438	645	340
514	988	2070	4236	5882	4151	2018	965	504	288
366	600	980	1453	1695	1438	965	590	360	227
251	364	509	649	708	645	504	360	248	171
173	229	290	341	361	340	288	227	171	127

TOTAL

Figure 9. Charge collection from a 200 MeV Fe ion at 0 degrees. (Si, 30 μ m pitch, 1 μ m depletion, 10 μ m diffusion)

Figure 10 shows model predictions of crosstalk to the nearest neighboring pixels for the case of a 30 μ m pitch Si pixel struck in the center with an ion at normal incidence.

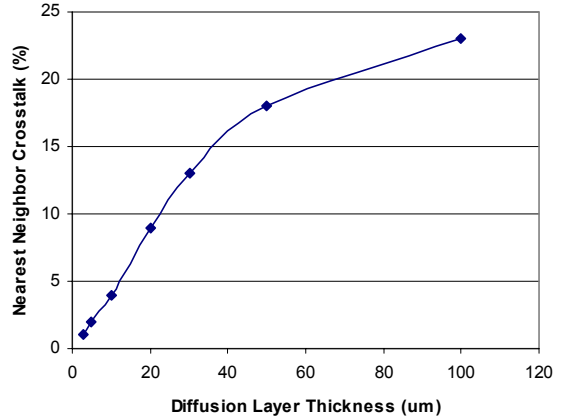


Figure 10. Model predictions of crosstalk as a function of diffusion layer thickness for a 30 micron pitch array of Si pixels.

6. CONCLUSIONS

A modeling program is underway to assess the potential impact of ionizing particle induced transients on the science mission of the NGST. A prototype model has been developed and preliminary transport analyses for materials of interest has been performed. Preliminary results indicate that the radiation effects problems are manageable. The transient assessment program will reduce the risk from the space radiation for the NGST mission.

REFERENCES

- [1] A.Claret, H.Dzitko and J.J.Engelmann, "Transient Particle Effects on the ISOCAM Instrument On-Board the Infrared Space Observatory," IEEE Trans. Nucl. Sci., Vol. 49, No. 6, p. 1511, December 1999.
- [2] J.L.Barth, J.C. Isaacs, and C. Poivey, "The Radiation Environment for the Next Generation Space Telescope," NGST Document 570, September 2000.
- [3] T.S.Lomheim, R.M.Shima, J.R.Angione, W.F.Woodward, D.J.Asman, R.A.Keller and L.W.Schumann, "Imaging Charge-Coupled Device (CCD) Transient Response to 17 and 50 MeV Proton and Heavy Ion Irradiation," IEEE Trans. Nucl. Sci., Vol. 37, No. 6, p. 1876, December 1990.
- [4] T.E.Dutton, W.F.Woodward and T.S.Lomheim, "Simulation of Proton-Induced transients on Visible and Infrared Focal Plane Arrays in a Space Environment, SPIE, Vol. 3063, p.77, 1997.
- [5] J.F.Ziegler, J.P.Biersack and U.Littmark, "The Stopping and Range of Ions in Solids," Pergamon Press, 1985.

- [6] T.M.Jordan, "An Adjoint Charged Particle Transport Method," IEEE Trans. Nucl. Sci., Vol. 23, 1976.
- [7] S.Kirkpatrick, "Modeling Diffusion and Collection of Charge from Ionizing Radiation in Silicon Devices," IEEE Trans. Elec. Dev., Vol. ED-26, p. 1742, 1979.

Jim Pickel serves as a consultant to industry and government in the field of radiation effects on microelectronics. He was one of the original researchers in the field of single event effects and developed the first single event upset (SEU) rate prediction models. He developed one of the first models for predicting gamma-induced noise in infrared detectors. He also performed pioneering work in understanding basic mechanisms and hardening of infrared (IR) detectors and cryogenic microelectronics. He has worked on developing procedures for evaluation of reliability of cryogenic electronics and in technology development for IR focal plane arrays. His recent work has included assessment of radiation effects for the Next Generation Space Telescope (NGST). He is a Fellow of the IEEE.

